Bioorganic & Medicinal Chemistry 19 (2011) 261–274

Contents lists available at ScienceDirect

Bioorganic & Medicinal Chemistry

journal homepage: www.elsevier.com/locate/bmc

# Inhibition of monoamine oxidase by selected C5- and C6-substituted isatin analogues

Clarina I. Manley-King, Jacobus J. Bergh, Jacobus P. Petzer *

*Pharmaceutical Chemistry, School of Pharmacy, North-West University, Private Bag X6001, Potchefstroom 2520, South Africa*

ARTICLE INFO

*Article history:*
Received 21 September 2010
Revised 3 November 2010
Accepted 9 November 2010
Available online 13 November 2010

*Keywords:*
Monoamine oxidase
Reversible inhibition
Selectivity
Competitive inhibition
Isatin
Molecular docking

ABSTRACT

Previous studies have shown that (*E*)-5-styrylisatin and (*E*)-6-styrylisatin are reversible inhibitors of human monoamine oxidase (MAO) A and B. Both homologues are reported to exhibit selective binding to the MAO-B isoform with (*E*)-5-styrylisatin being the most potent inhibitor. To further investigate these structure–activity relationships (SAR), in the present study, additional C5- and C6-substituted isatin analogues were synthesized and evaluated as inhibitors of recombinant human MAO-A and MAO-B. With the exception of 5-phenylisatin, all of the analogues examined were selective MAO-B inhibitors. The C5-substituted isatins exhibited higher binding affinities to MAO-B than the corresponding C6-substituted homologues. The most potent MAO-B inhibitor, 5-(4-phenylbutyl)isatin, exhibited an $IC_{50}$ value of 0.66 nM, approximately 13-fold more potent than (*E*)-5-styrylisatin and 18,500-fold more potent than isatin. The most potent MAO-A inhibitor was found to be 5-phenylisatin with an $IC_{50}$ value of 562 nM. The results document that substitution at C5 with a variety of substituents is a general strategy for enhancing the MAO-B inhibition potency of isatin. Possible binding orientations of selected isatin analogues within the active site cavities of MAO-A and MAO-B are proposed.



## 1. Introduction

Monoamine oxidase (MAO) A and B are flavin adenine dinucleotide (FAD) containing enzymes which are tightly anchored to the mitochondrial outer membrane.[1] Although MAO-A and MAO-B are encoded by separate genes, they share approximately 70% amino acid sequence identity.[2] The X-ray crystal structures of recombinant human MAO-A[3] and MAO-B[1] have shown that the active site amino acid residues and their relative geometries are also highly conserved between the 2 enzymes and only 6 of the 16 active site residues differ between the 2 isozymes.[3] Despite these similarities, the enzymes have unique substrate and inhibitor specificities. For example, MAO-A catalyses the oxidation of serotonin and norepinephrine and is irreversibly inhibited by clorgyline while MAO-B preferentially utilises benzylamine as substrate and is irreversibly inhibited by (*R*)-deprenyl. Both isoforms utilise dopamine as substrate.[4] In addition, literature reports a variety of small molecule inhibitors with selectivities towards the two enzymes ranging from negligible to several orders of a magnitude.[5,6]

Because MAO-A and MAO-B catalyses the catabolism of neurotransmitter amines, they are considered attractive drug targets in the therapy of neurological disorders. Both reversible and irreversible inhibitors of MAO-A are used to treat depressive illness and anxiety disorder. The antidepressant effect of MAO-A inhibitors are dependent on the inhibition of the catabolism of serotonin, norepinephrine and dopamine in the brain which leads to increased levels of these neurotransmitters.[4] MAO-A inhibitors are particularly effective in the treatment of depression in elderly patients.[4,7] Inhibitors of MAO-B are employed in the treatment of neurodegenerative disorders such as Parkinson's disease (PD). MAO-B appears to be the major dopamine metabolizing enzyme in the basal ganglia, and inhibitors of this enzyme may conserve the depleted dopamine stores in the PD brain. This may lead to enhanced dopaminergic neurotransmission and consequently symptomatic relief of the symptoms of PD.[8–10] MAO-B inhibitors may also increase the elevation of dopamine levels in the basal ganglia following levodopa treatment[11] and are therefore used as adjuvant to levodopa therapy in PD.[12] Besides providing symptomatic relief, MAO-B inhibitors may also protect against further neurodegeneration in PD by reducing the levels of potentially toxic byproducts such as $H_2O_2$ and dopaldehyde which form as a result of the oxidative metabolism of dopamine.[13] MAO-B inhibitors may be particularly relevant in the therapy in age-related neurodegenerative disorders such as PD since MAO-B activity and density increase in most brain regions with age.[14,15]

The endogenous small molecule inhibitor isatin (**1**) (Fig. 1) is reported to be a reversible inhibitor of both human MAO-A and MAO-B with enzyme–inhibitor dissociation constants ($K_i$ values) of 15 μM and 3 μM for the two isozymes, respectively.[16] The three-dimensional structure of recombinant human MAO-B with isatin bound to the active site shows that isatin is located in the

* Corresponding author. Tel.: +27 18 2992206; fax: +27 18 2994243.
*E-mail address:* jacques.petzer@nwu.ac.za (J.P. Petzer).

0968-0896/$ - see front matter © 2010 Elsevier Ltd. All rights reserved.
doi:10.1016/j.bmc.2010.11.028

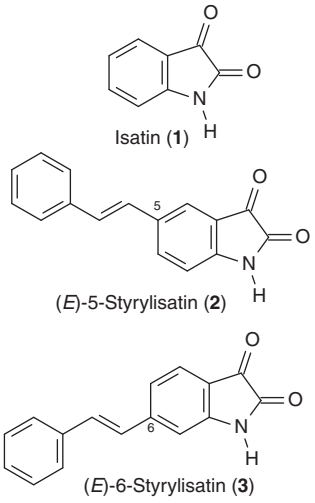


**Figure 1.** The structures of isatin (**1**), (*E*)-5-styrylisatin (**2**) and (*E*)-6-styrylisatin (**3**).

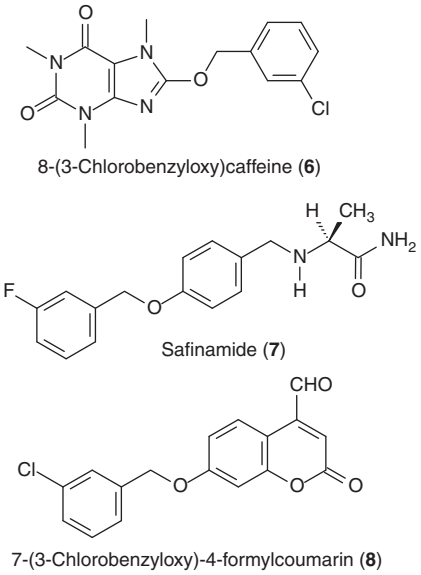


**Figure 3.** The structures of 8-(3-chlorobenzyloxy)caffeine (**6**), safinamide (**7**) and 7-(3-chlorobenzyloxy)-4-formylcoumarin (**8**).

substrate cavity in close proximity to the FAD co-factor where it is involved in hydrogen bonding with conserved water molecules.[17] Since isatin binds within the substrate cavity, the entrance cavity of the enzyme is unoccupied. Based on this observation we have recently synthesized (*E*)-5-styrylisatin (**2**) and (*E*)-6-styrylisatin (**3**) in an attempt to enhance the binding affinity of isatin to MAO-B.[18] The results documented that both (*E*)-styrylisatin analogues exhibited significantly higher binding affinities than isatin with the C5-substituted isomer being the more potent inhibitor of the two isomers. Modelling studies suggested that the (*E*)-styrylisatin analogues binds to the MAO-B active site with the isatin dioxoindolyl ring bound to the substrate cavity while the styryl side chain extends into the entrance cavity. The interaction of the styryl side chain with the entrance cavity amino acid residues may allow for more productive binding with the enzyme compared to isatin and hence more potent inhibition.[18] In accordance with this analysis the small molecule caffeine (**4**) (Fig. 2), which is expected to bind to either the substrate or entrance cavity, is a weak MAO-B inhibitor with a $K_i$ value of 3.6 mM.[18] The C8 chlorostyryl substituted analogue, (*E*)-8-(3-chlorostyryl)caffeine [CSC, (**5**)], however was found to be a potent reversible inhibitor with a $K_i$ value of 0.086 μM.[19,20] The higher affinity of CSC for the MAO-B active site may be explained by the additional productive interactions of the chlorostyryl side chain within the entrance cavity.

We have recently shown that the MAO-B binding affinity of caffeine may also be enhanced by substitution with a variety of benzyloxy side chains at C8 of the caffeine ring.[21] For example, 8-(3-chlorobenzyloxy)caffeine (**6**) (Fig. 3) inhibits recombinant

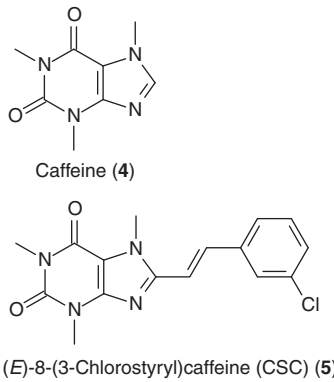


**Figure 2.** The structures of caffeine (**4**) and (*E*)-8-(3-chlorostyryl)caffeine [CSC, (**5**)].

human MAO-B with a $K_i$ value of 0.036 μM, approximately $10^5$-fold more potently than caffeine. Modelling studies have shown that the caffeine ring is located within the substrate cavity of the enzyme while the benzyloxy side chain binds within the entrance cavity. Again, the improved inhibition of the 8-benzyloxycaffeiene analogues compared to caffeine may be explained by binding interactions between the benzyloxy side chain and the entrance cavity of MAO-B. The view that the benzyloxy side chain binds within the entrance cavity is supported by the three-dimensional structure of a complex between safinamide (**7**) and recombinant human MAO-B which shows that the 3-fluorobenzyloxy side chain of safinamide occupies the entrance cavity while the propanamidyl moiety is located within the substrate cavity.[22] Similarly, the structure of a complex between 7-(3-chlorobenzyloxy)-4-formylcoumarin (**8**) and human MAO-B shows that the 3-chlorobenzyloxy side chain binds in the entrance cavity of the enzyme with the coumarin ring occupying the substrate cavity.[22]

While the three-dimensional complex between isatin and MAO-A has not yet been determined, modelling studies have been performed with (*E*)-5-styrylisatin (**2**) and (*E*)-6-styrylisatin (**3**).[18] These suggest that, similar to its binding mode within MAO-B, the dioxoindolyl rings of both isomers occupy the space in close proximity to the FAD co-factor with their respective styryl side chains extending towards the entrance of the active site. Notably, (*E*)-5-styrylisatin exhibited a 19-fold higher binding affinity to MAO-A than isatin while the C6-substituted isomer (**3**) had a similar binding affinity to that of isatin.[18] The lack of enhancement of the MAO-A binding affinity by C6 styryl substitution is not well understood.

To further investigate these structure–activity relationships (SAR), in the present study, we have synthesized additional C5- and C6-substituted isatin analogues and evaluated them as inhibitors of recombinant human MAO-A and MAO-B. One of the goals of this study was to determine if C5-substituted isatin analogues are in general better MAO-B inhibitors than the corresponding C6 isomers as observed with the (*E*)-styrylisatin analogues. Furthermore, this study also aimed to determine the effect of C5- and C6-substitution of isatin on MAO-A inhibition activity. As discussed above, compared to isatin, (*E*)-5-styrylisatin (**2**) was found to be a better MAO-A inhibitor while the C6-substituted isomer (**3**) had a similar inhibition potency to that of isatin.[18] Among the

C5- and C6-substituents chosen for this study was the benzyloxy side chain which has been shown to enhance the binding affinity of caffeine to the active site of both MAO-A and MAO-B.[21] Other substituents considered in this study include the phenoxy, 2-phenylethyl, 4-phenylbutyl, phenyl and 4-chlorophenoxy groups. We have also examined the importance of the isatin moiety for binding to MAO-A and MAO-B by comparing the inhibition potencies of the C5- and C6-substituted isatins with those of the corresponding aniline analogues. With this comparison the importance of the carbonyl functional groups of the dioxoindolyl ring for binding to the MAO isozymes may be determined. Literature reports that the NH and the C2 carbonyl oxygen of isatin are hydrogen bonded to water molecules in the substrate cavity of MAO-B.[17] Similar interactions may also be possible between the aniline $NH_2$ and the active sites of the MAO enzymes.

## 2. Results

### 2.1. Chemistry

In the present study a series of 10 C5- and C6-substituted isatin analogues (**9a**–**j**) were synthesized with the aim of examining their MAO inhibitory properties. The C5-substituted isatin analogues (**9a**, **c**, **e**, **g**, **i**, **j**) were synthesized by treating the appropriately C4-substituted aniline (**10a**, **c**, **e**, **g**, **i**, **j**) with diethyl ketomalonate in the presence of acetic acid according to the literature description (Scheme 1).[23] The C6-substituted isatin analogues (**9b**, **d**, **f**, **h**) were similarly synthesized, from the C3-substituted aniline derivatives (**10b**, **d**, **f**, **h**) and diethyl ketomalonate. While the latter reaction may also give the corresponding C4-substituted isatin analogues, only a single product was isolated from the reaction mixtures. $^1$H NMR indicated that in each instance these were the C6-substituted analogues as evidenced by the singlet corresponding to the C4 proton (**9b**, 6.46 ppm; **9d**, 6.61 ppm; **6f**, 6.28 ppm; **9h**, 7.09 ppm). This is in accordance to the literature report that the reaction between C3-substituted aniline derivatives and diethyl ketomalonate yields the corresponding C6-substituted isatins.[23] Furthermore, the molecular structure of **9d** was elucidated by X-ray crystallography and confirms substitution at the C6 position (Fig. 4). Although the target compounds were obtained in low yields (1.2–9.3%) the crystalline products were of a high degree of purity as judged by HPLC (see Section 4). These low yields may be due to resinification and the formation of side products. Fortunately, the desired isatins could be obtained via a combination of filtration steps, adjusting

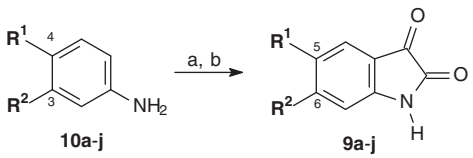


10a-j 9a-j

| | $R^1$ | $R^2$ |
|---|---|---|
| **a** | $C_6H_5CH_2O$ | H |
| **b** | H | $C_6H_5CH_2O$ |
| **c** | $C_6H_5CH_2CH_2$ | H |
| **d** | H | $C_6H_5CH_2CH_2$ |
| **e** | $C_6H_5O$ | H |
| **f** | H | $C_6H_5O$ |
| **g** | $C_6H_5$ | H |
| **h** | H | $C_6H_5$ |
| **i** | $C_6H_5(CH_2)_4$ | H |
| **j** | 4-$ClC_6H_4O$ | H |

**Scheme 1.** Synthetic route to C5- and C6-substituted isatin analogues (**9a**–**j**). Reagents and conditions: (a) diethyl ketomalonate, $CH_3CO_2H$, 120 °C; (b) air, 120 °C.

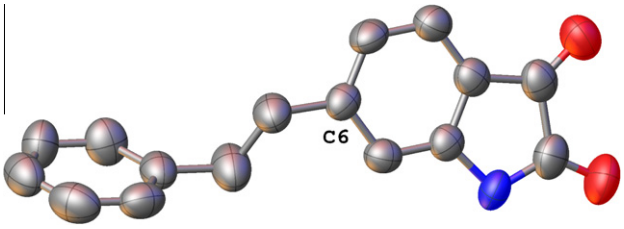


**Figure 4.** The X-ray crystallographic structure of **9d** shown with displacement ellipsoids.

the pH of the filtrates to 3 and then <1 and column chromatography (see Section 4). While the Sandmeyer methodology is more frequently used for the synthesis of isatin analogues, the low solubility of the starting anilines in the aqueous reaction medium made this procedure unsuitable for the synthesis of the target isatin analogues.[24] The successful formation of the isatin ring system of the target compounds were verified by the presence of a $^{13}$C NMR signal at 181–185 ppm which corresponds to carbonyl C3 and a signal at 159–161 ppm which corresponds to carbonyl C2 (Table 1).[25]

With the exception of 4-(2-phenylethyl)aniline (**10c**), 3-(2-phenylethyl)aniline (**10d**) and 4-(4-phenylbutyl)aniline (**10i**) all of the anilines required for the synthesis of the isatin analogues were commercially available. Anilines **10c** and **10d** were synthesized by reacting diethyl 4- or diethyl 3-nitrobenzylphosphonate (**11a**, **b**)[26] with benzaldehyde (**12**) to yield the 4- or 3-nitrostilbenes (**13a**, **b**), respectively (Scheme 2).[27] Catalytic hydrogenation of the nitrostilbenes in the presence of Pd/C yielded the corresponding anilines (**10c**, **d**). Aniline **10i** was similarly synthesized by reacting diethyl 4-nitrobenzylphosphonate (**11a**) with cinnamaldehyde (**14**) to obtain 1-nitro-4-[(1*E*,3*E*)-4-phenylbuta-1,3-dien-1-yl]benzene (**15**). Again, hydrogenation of **15** afforded the corresponding aniline **10i**.

### 2.2. MAO inhibition studies—isatin analogues

To determine the MAO-A and MAO-B inhibition potencies of the test inhibitors, the extent by which different concentrations of a test inhibitor reduces the rate of the MAO-catalysed oxidation of kynuramine, a mixed MAO-A/B substrate, was measured. For this purpose the recombinant human MAO-A and MAO-B enzymes were employed.[28] Kynuramine is non-fluorescent until undergoing

**Table 1**
$^{13}$C NMR chemical shifts for carbonyl C2 and C3 of isatin derivatives **9a**–**j**[a]

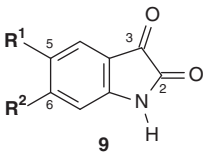


9

| | $R^1$ | $R^2$ | C2 | C3 |
|---|---|---|---|---|
| **9a** | $C_6H_5CH_2O$ | H | 159.5 | 184.6 |
| **9b** | H | $C_6H_5CH_2O$ | 160.5 | 181.5 |
| **9c** | $C_6H_5CH_2CH_2$ | H | 159.5 | 184.5 |
| **9d** | H | $C_6H_5CH_2CH_2$ | 159.9 | 183.7 |
| **9e** | $C_6H_5O$ | H | 159.6 | 184.1 |
| **9f** | H | $C_6H_5O$ | 160.1 | 181.8 |
| **9g** | $C_6H_5$ | H | 159.6 | 184.4 |
| **9h** | H | $C_6H_5$ | 159.8 | 183.7 |
| **9i** | $C_6H_5(CH_2)_4$ | H | 159.5 | 184.6 |
| **9j** | 4-$ClC_6H_4O$ | H | 159.5 | 184.0 |

[a] The NMR experiments were conducted in DMSO-$d_6$ (see Section 4).

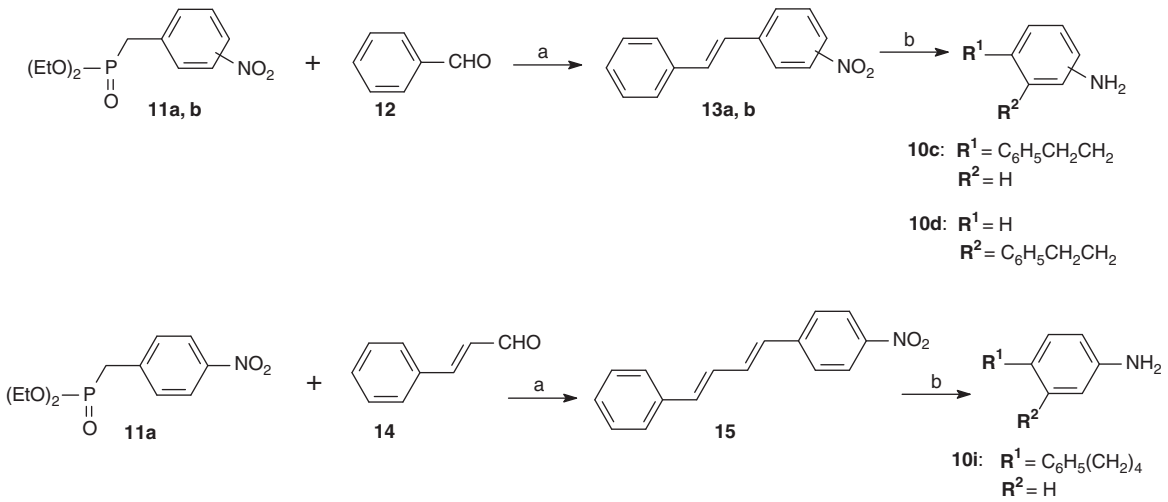


**Scheme 2.** Synthetic route to aniline derivatives **10c**, **10d** and **10i**. Reagents and conditions: (a) NaOEt; (b) $H_2$ (atm), Pd/C (10%), rt.

MAO-catalysed oxidative deamination and subsequent ring closure to yield 4-hydroxyquinoline, a fluorescent metabolite. The concentrations of the MAO-generated 4-hydroxyquinoline in the incubation mixtures was determined by comparing the fluorescence emitted by the samples to that of known amounts of authentic 4-hydroxyquinoline.[28] At the excitation (310 nm) and emission (400 nm) wavelengths and inhibitor concentrations used in this study, none of the test inhibitors fluoresced or quenched the fluorescence of 4-hydroxyquinoline. The inhibition potencies of the test inhibitors were expressed as the $IC_{50}$ values (Fig. 5). To allow for the calculation of the selectivity index [SI = $K_i$(MAO-A)/$K_i$(-MAO-B)], the experimentally determined $IC_{50}$ values were converted to the corresponding $K_i$ values for the inhibition of MAO-A and MAO-B according to the Cheng–Prusoff equation.[20,29]

The $IC_{50}$ values for the inhibition of MAO-A and -B by isatin analogues **9a**–**j** are presented in Table 2. For comparison, the inhibition potencies of isatin (**1**), (*E*)-5-styrylisatin (**2**) and (*E*)-6-styrylisatin (**3**) were also measured and are given in Table 2. The MAO-A and -B inhibition potencies of compounds **1**–**3** have been previously reported using the purified recombinant human enzymes which were expressed in *Pichia pastoris*.[16,18] The present account reports the inhibition data using membrane bound recombinant human MAO-A and -B from insect cells. In accordance with the literature, isatin was found to be a moderately potent inhibitor of MAO-A and -B with $IC_{50}$ values of 31.8 μM and 12.4 μM, respectively. Based on the selectivity index (Table 2) isatin is approximately 1.57-fold more selective for MAO-B than for the A isoform. Also in agreement with the literature[18] was the finding that (*E*)-5-styrylisatin (**2**) is a potent inhibitor of both MAO-A and -B with $IC_{50}$ values of 0.233 μM and 0.009 μM, respectively. In fact, (*E*)-5-styrylisatin was the second most potent MAO-B inhibitor examined in this study and approximately 1300-fold more potent than was isatin. Also in agreement with literature,[18] (*E*)-6-styrylisatin was a relatively potent MAO-B inhibitor, while exhibiting moderately potent MAO-A inhibitory activity. Compared to the C5-substituted isomer **2**, (*E*)-6-styrylisatin was approximately 68-fold less potent as an MAO-B inhibitor.

The most potent MAO-B inhibitor among the examined compounds was 5-(4-phenylbutyl)isatin (**9i**) with an $IC_{50}$ value of 0.66 nM, approximately 13-fold more potent than (*E*)-5-styrylisatin and 18,500-fold more potent than isatin. The observation that the 4-phenylbutyl group is the longest side chain considered in this study indicates that longer side chains enhance the MAO-B inhibition potency of isatin to a larger extent compared to relatively

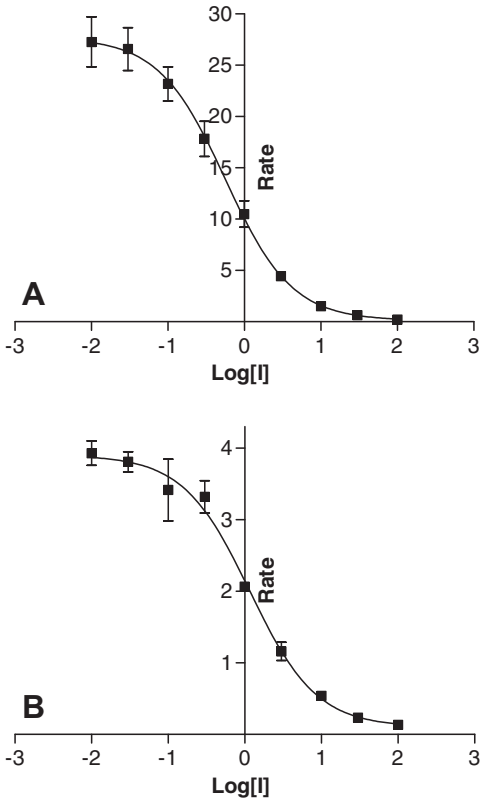


**Figure 5.** The sigmoidal dose–response curve of the initial rates of oxidation of kynuramine by recombinant human MAO-A (Panel A) and recombinant human MAO-B (Panel B) versus the logarithm of concentration of inhibitor **9g** (expressed in nM). The determinations were carried out in duplicate and the values are expressed as the mean ± SD. The concentrations of kynuramine used were 45 μM and 30 μM for the studies with MAO-A and MAO-B, respectively, and the rate data are expressed as nmol 4-hydroxyquinoline formed/min/mg protein.

shorter side chains. In contrast to its effect on the MAO-B inhibition potency, the 4-phenylbutyl side chain did not enhance the MAO-A inhibition potency of isatin to a great extent. Compound **9i** only moderately inhibited MAO-A with an $IC_{50}$ value of 2.19 μM, approximately 14-fold more potent than the MAO-A inhibition potency of isatin. The only isatin analogues examined in this study which potently inhibited MAO-A were (*E*)-5-styrylisatin (**2**) and

**Table 2**
The $IC_{50}$ values and calculated $K_i$ values for the inhibition of recombinant human MAO-A and -B by isatin derivatives **9a**–**j**[a]

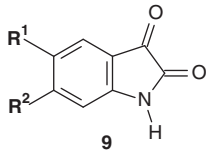


9

| | $IC_{50}$ (μM) | | | | $K_i$[b] (μM) | | SI[c] |
|---|---|---|---|---|---|---|---|
| | $R^1$ | $R^2$ | MAO-A | MAO-B | MAO-A | MAO-B | |
| **9a** | $C_6H_5CH_2O$ | H | 4.62 ± 0.148 | 0.103 ± 0.011 | 1.22 | 0.044 | 27.4 |
| **9b** | H | $C_6H_5CH_2O$ | 72.4 ± 26.3 | 0.138 ± 0.005 | 19.1 | 0.059 | 321 |
| **9c** | $C_6H_5CH_2CH_2$ | H | 4.88 ± 2.03 | 1.40 ± 0.124 | 1.29 | 0.603 | 2.13 |
| **9d** | H | $C_6H_5CH_2CH_2$ | 6.93 ± 0.842 | 9.93 ± 4.54 | 1.83 | 4.28 | 0.427 |
| **9e** | $C_6H_5O$ | H | 9.44 ± 0.356 | 1.54 ± 0.575 | 2.49 | 0.663 | 3.75 |
| **9f** | H | $C_6H_5O$ | 62.2 ± 8.25 | 9.91 ± 0.752 | 16.4 | 4.27 | 3.84 |
| **9g** | $C_6H_5$ | H | 0.562 ± 0.026 | 1.19 ± 0.173 | 0.148 | 0.513 | 0.289 |
| **9h** | H | $C_6H_5$ | 4.64 ± 0.556 | 8.52 ± 0.260 | 1.22 | 3.67 | 0.333 |
| **9i** | $C_6H_5(CH_2)_4$ | H | 2.19 ± 0.218 | 0.00066 ± 0.00001 | 0.577 | 0.00028 | 2030 |
| **9j** | 4-$ClC_6H_4O$ | H | 12.2 ± 1.22 | 0.066 ± 0.008 | 3.21 | 0.028 | 113 |
| Isatin | H | H | 31.8 ± 4.50 | 12.4 ± 0.693 | 8.38 | 5.34 | 1.57 |
| **2** | (*E*)-$C_6H_5CH{=}CH$ | H | 0.233 ± 0.006 | 0.009 ± 0.001 | 0.061 | 0.004 | 15.8 |
| **3** | H | (*E*)-$C_6H_5CH{=}CH$ | 2.72 ± 0.082 | 0.617 ± 0.011 | 0.717 | 0.266 | 2.70 |

[a] All values are expressed as the mean ± SD of duplicate determinations.
[b] The $K_i$ values were calculated from the experimentally measured $IC_{50}$ values according to the equation by Cheng and Prusoff: $K_i = IC_{50}/(1 + [S]/K_m)$ with [S] = 45 μM and $K_m$ (kynuramine) = 16.1 μM for human MAO-A and [S] = 30 μM and $K_m$ (kynuramine) = 22.7 μM for human MAO-B.[21,29]
[c] The selectivity index is the selectivity for the MAO-B isoform and is given as the ratio of $K_i$(MAO-A)/$K_i$(MAO-B).

(*E*)-5-phenylisatin (**9g**) with $IC_{50}$ values of 0.233 μM and 0.562 μM, respectively. The other homologues examined all exhibited $IC_{50}$ values towards MAO-A in the μM range. Interestingly, compounds **2** and **9g** are the only C5-substituted isatin analogues with a side chain phenyl ring, that is, conjugated to the isatin ring system. Also noteworthy is the observation that the majority (seven) of the isatin analogues examined displayed selectivity for the MAO-B isoform (Table 2).

The C5- and C6-benzyloxy substituted isatin analogues (**9a**, **b**) were also found to be potent MAO-B inhibitors with $IC_{50}$ values of 0.103 μM and 0.138 μM, respectively. As stated in the Introduction, this finding is in agreement with literature reports that the benzyloxy side chain enhances the binding affinity of small molecules such as caffeine to the active site of MAO-B.[21] Interestingly, the C6-benzyloxy substituted analogue **9b** was the weakest MAO-A inhibitor among the isatin analogues.

Compared to the benzyloxy substituted isatin analogues (**9a**, **b**), 5-(2-phenylethyl)isatin (**9c**) and 6-(2-phenylethyl)isatin (**9d**) were relatively weaker MAO-B inhibitors with $IC_{50}$ values of 1.40 μM and 9.93 μM, respectively. Compounds **9c** was approximately 13-fold less potent that the corresponding C5-benzyloxy substituted isatin analogues (**9a**) while **9d** was approximately 71-fold less potent than the corresponding C6-benzyloxy substituted isatin analogue **9b**. Similarly, 5-phenoxyisatin (**9e**), 6-phenoxyisatin (**9f**), 5-phenylisatin (**9g**) and 6-phenylisatin (**9h**) were also found to be relatively weaker MAO-B inhibitors than the benzyloxy substituted analogues (**9a**, **b**). It can therefore be concluded that the 2-phenylethyl, phenoxy and phenyl side chains do not increase the MAO-B binding affinity of isatin to the same extent observed for the (*E*)-styryl and benzyloxy side chains.

While 5-phenoxyisatin (**9e**) was found to be moderately potent MAO-B inhibitor ($IC_{50}$ = 1.54 μM), the C5-substituted 4-chlorophenoxy analogue **9j** proved to be a potent MAO-B inhibitor with an $IC_{50}$ value of 0.066 μM. This result demonstrates the ability of halogen substitution at a side chain phenyl ring to enhance binding affinity of reversible inhibitors to MAO-B. This effect is similar to that observed for 8-benzyloxycaffeinyl,[21] (*E*)-8-styrylcaffeinyl[19] and (*E*)-2-styrylbenzimidazolyl analogues.[30] For example, 8-(3-chlorobenzyloxy)caffeine is reported to inhibit human MAO-B with an $IC_{50}$ value of 0.107 μM, approximately 16-fold more potently than the unsubstituted analogue, 8-benzyloxycaffeine, with an $IC_{50}$ value of 1.77 μM.[21]

### 2.3. MAO inhibition studies—aniline analogues

As mentioned in Section 1, the importance of the isatin moiety for binding to MAO-A and MAO-B was also examined by comparing the inhibition potencies of the C5- and C6-substituted isatins with those of the corresponding *para*- and *meta*-substituted anilines. Inspection of the X-ray crystal structure of isatin in complex with human MAO-B suggests that the dioxoindolyl NH and the C2 carbonyl oxygen are involved in stabilizing hydrogen bond interactions with water molecules in the substrate cavity of MAO-B.[17] Since similar interactions may also be possible between the aniline $NH_2$ and the active sites of the MAO enzymes, the anilines may also possess MAO inhibitory properties. By comparing the MAO inhibition potencies of the isatins with those of the anilines, the importance of the lactam and C2 carbonyl functional groups of the dioxoindolyl ring for binding to the MAO isozymes may be evaluated.

The $IC_{50}$ values for the inhibition of recombinant human MAO-A and -B by the aniline analogues (**10a**–**l**) are presented in Table 3. All of the anilines evaluated were found to be relatively weak MAO-A inhibitors with the most potent compound (**10k**) exhibiting an $IC_{50}$ value of 25.3 μM. The anilines were also relatively weak MAO-B inhibitors with the most potent inhibitor, the 4-phenylbutyl substituted aniline (**10i**), exhibiting an $IC_{50}$ value of 5.55 μM. With the exception of **10c**, **10e** and **10h**, all of the anilines examined displayed selectivity for the MAO-B isoform (Table 3). This isoform selectivity is similar to that observed for the isatin analogues.

Interestingly, the 4-phenylbutyl substituted isatin analogue was also the most potent MAO-B inhibitor among the isatin analogues. Inspection of the inhibition data in Tables 2 and 3 shows

**Table 3**
The $IC_{50}$ values and calculated $K_i$ values for the inhibition of recombinant human MAO-A and -B by aniline derivatives **10a–l**[a]

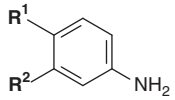


**10**

| | $IC_{50}$ (μM) | | | | $K_i$[b] (μM) | | SI[c] |
|---|---|---|---|---|---|---|---|
| | $R^1$ | $R^2$ | MAO-A | MAO-B | MAO-A | MAO-B | |
| **10a** | $C_6H_5CH_2O$ | H | 191 ± 53.5 | 12.8 ± 4.47 | 50.3 | 5.51 | 9.13 |
| **10b** | H | $C_6H_5CH_2O$ | 466 ± 75.2 | 23.4 ± 5.65 | 123 | 10.1 | 12.2 |
| **10c** | $C_6H_5CH_2CH_2$ | H | 131 ± 6.22 | 135 ± 0.011 | 34.5 | 58.1 | 0.594 |
| **10d** | H | $C_6H_5CH_2CH_2$ | 355 ± 38.8 | 115 ± 7.85 | 93.5 | 49.5 | 1.89 |
| **10e** | $C_6H_5O$ | H | 91.4 ± 21.1 | 303 ± 8.77 | 24.1 | 131 | 0.185 |
| **10f** | H | $C_6H_5O$ | No inhibition[d] | 140 ± 42.1 | — | 60.3 | — |
| **10g** | $C_6H_5$ | H | No inhibition[d] | No inhibition[d] | — | — | — |
| **10h** | H | $C_6H_5$ | 68.6 ± 1.32 | No inhibition[d] | 18.1 | — | — |
| **10i** | $C_6H_5(CH_2)_4$ | H | No inhibition[d] | 5.55 ± 0.492 | — | 2.39 | — |
| **10j** | 4-$ClC_6H_4O$ | H | 29.3 ± 1.33 | 16.8 ± 1.74 | 7.72 | 7.24 | 1.07 |
| **10k** | (*E*)-$C_6H_5CH{=}CH$ | H | 25.3 ± 2.01 | 6.34 ± 3.41 | 6.67 | 2.73 | 2.44 |
| **10l** | H | (*E*)-$C_6H_5CH{=}CH$ | 30.4 ± 4.70 | 5.74 ± 1.05 | 8.01 | 2.47 | 3.24 |

[a] All values are expressed as the mean ± SD of duplicate determinations.
[b] The $K_i$ values were calculated from the experimentally measured $IC_{50}$ values according to the equation by Cheng and Prusoff: $K_i = IC_{50}/(1 + [S]/K_m)$ with [S] = 45 μM and $K_m$ (kynuramine) = 16.1 μM for human MAO-A and [S] = 30 μM and $K_m$ (kynuramine) = 22.7 μM for human MAO-B.[21,29]
[c] The selectivity index is the selectivity for the MAO-B isoform and is given as the ratio of $K_i$(MAO-A)/$K_i$(MAO-B).
[d] No inhibition observed at a maximum tested concentration of 100 μM.

that the order of the MAO-B inhibition potencies of the aniline analogues is similar to that of the isatin analogues. For example, the aniline analogues substituted with styryl, benzyloxy and 4-chlorophenoxy side chains at the *para*- and *meta*-positions were more potent MAO-B inhibitors than the corresponding 2-phenylethyl, phenoxy and phenyl substituted anilines. Similarly, the C5- and C6-substituted styryl, benzyloxy and 4-chlorophenoxy isatin analogues were more potent MAO-B inhibitors than the corresponding 2-phenylethyl, phenoxy and phenyl substituted isatins. These data suggests that the isatin and aniline analogues exhibit similar binding modes to the active site of MAO-B. Previous modelling studies[18] have suggested that (*E*)-5-styrylisatin (**2**) and (*E*)-6-styrylisatin (**3**) bind to the MAO-B active site with the dioxoindolyl rings of both isomers occupying the substrate cavity space in close proximity to the FAD co-factor while their respective styryl side chains extends towards the entrance cavity of the enzyme. Should the aniline analogues exhibit as similar binding mode, the aniline moiety is expected to also occupy the relatively polar substrate cavity[31] where the $NH_2$ may be involved in hydrogen bond interactions. The *para*- and *meta*-substituted side chains are expected to extend towards the entrance cavity of the enzyme. By employing molecular docking studies, possible binding modes and interactions of selected aniline and isatin analogues within an MAO-B active site model will be proposed below.

The finding that the aniline analogues are weaker MAO-A and -B inhibitors than the corresponding isatin analogues indicates that the lactam and C2 carbonyl functional groups of the dioxoindolyl ring are important structural features for binding to the MAO active sites. A possible explanation may be that the dioxoindolyl carbonyl oxygens act as hydrogen bond acceptors within the substrate cavities of MAO-A and -B thereby providing additional stabilization of the inhibitor–enzyme complex. In accordance with this proposal, the three-dimensional structure of isatin bound to human MAO-B has shown the C2 carbonyl oxygen to be hydrogen bonded to ordered water molecules in the substrate cavity.[17] While the structure of isatin bound to MAO-A has not yet been determined the architectures of the MAO-A and -B active sites are similar,[3] especially in the vicinity of the FAD co-factor where hydrogen bonding between isatin and MAO-B occur. It is therefore reasonable to propose that the carbonyl oxygen of isatin and C5- and C6-substituted isatin analogues also may act as hydrogen bond acceptors in the MAO-A active site. Since the aniline analogues examined here do not possess carbonyl functional groups they lack the additional stabilizing interactions with the MAO active sites that these functional groups provide and are hence weaker inhibitors than the isatins. Another factor that may contribute to stabilizing isatins, and not anilines, within the active sites of MAO-A and -B are possible π–π stacking interactions between the dioxoindolyl ring and the amide of an active site Gln residue. In MAO-A, Gln-215 is reported to undergo stacking interactions with harmine[3] while in MAO-B Gln-206 may similarly interact with bound ligands.

Since both aniline and isatin are expected to be uncharged in the buffer used for the inhibition studies (pH 7.4), differing ionisation states of the aniline $NH_2$ and isatin lactam NH do not explain the difference in binding affinities to the MAO enzymes. Also, since aminyl substrates of MAO are reported to bind as the deprotonated amines to the active sites of these enzymes, it may be expected that the uncharged aniline and isatin species are the active inhibitors.[11,32]

## 2.4. Reversibility studies

With the finding that a several C5- and C6-substituted isatin analogues are potent MAO-A and -B inhibitors, this study further aimed to investigate whether the observed enzyme inhibition is reversible or irreversible. For this purpose the time dependence of MAO-A and -B inhibition by one representative inhibitor, compound **9c**, was evaluated. The MAO-A and -B inhibition potencies of compound **9c** are relatively lower compared to other isatin analogues evaluated in this study. Since these studies are conducted at concentrations equal to the $IC_{50}$ values of the test compound, this would allow for the use of relatively higher inhibitor concentrations compared to the concentrations that would be needed for more potent compounds. A possible hydrolysis event (see below) is expected to have a smaller effect (over the 60 min experimental time) on higher concentrations of an inhibitor and would yield results that are better interpretable. Recombinant human MAO-B

was preincubated with **9c** for periods of 0, 15, 30 and 60 min and the residual rates of the MAO-A and -B catalysed oxidation of kynuramine were measured. For this purpose, the concentrations of **9c** chosen were 9.76 μM for the incubations with MAO-A and 2.80 μM for the incubations with MAO-B. These concentrations are approximately twofold the measured $IC_{50}$ values for the inhibition of the respective enzymes by **9c**.

As shown in Figure 6A and B, there is no time-dependent reduction in the rates of MAO-A and -B catalysed oxidation of kynuramine when compound **9c** is preincubated with the enzyme for various periods of time. From this result it may be concluded that the inhibition of MAO-A and -B is reversible, at least for the time period (60 min) and at the inhibitor concentrations ($2 \times IC_{50}$) evaluated. Interestingly, marked increases of both the MAO-A and -B catalytic rate with increased preincubation time of **9c** with the enzymes are observed. One possible explanation for this observation is that **9c**, and probably the other isatin analogues, undergo slow hydrolysis in the aqueous buffer (pH 7.4) used for the inhibition studies. Isatins are known to undergo C–N bond fission to yield the ring-opened amino acid. This process is reversible and acidification reforms the isatin.[33] Considering that an incubation time of 20 min was chosen for determining the inhibition potencies of the isatin analogues, the recorded $IC_{50}$ values (Table 2) may be an underestimation of the MAO-A and -B inhibition potencies. Since relatively little loss of inhibition potency of the isatin analogues is observed between the 15 min and 30 min time points, the effect of hydrolysis on the measured $IC_{50}$ values is expected to be relatively small. Time-dependent inhibition studies with other isatin analogues yielded similar results (data not shown).

To further examine the modes of MAO-A and -B inhibition, sets of Lineweaver–Burk plots were constructed for the inhibition of both enzymes by **9c**, the selected representative inhibitor (Fig. 7A and B). Inspection of the Lineweaver–Burk plots suggests that **9c** inhibits both MAO-A and -B competitively since the plots are linear and intersect at the *y*-axis. These findings lend further support for the finding that **9c** interacts reversibly with the active sites of human MAO-A and -B and is in accordance with literature which reports that both isatin[16] and (*E*)-styrylisatin analogues[18] are competitive inhibitors of recombinant human MAO-A and -B.

## 2.5. Molecular modelling studies

The findings of this study show that while the isatin analogues are in general good MAO-A and -B inhibitors, the corresponding aniline analogues act as weak inhibitors. As discussed above, one possible reason for this observation is that, in addition to the potential hydrogen bonding interactions provided by the lactam nitrogen, the isatin carbonyl oxygens may interact via hydrogen bonding with MAO-A and -B active site residues and water molecules in the vicinity of the FAD co-factor. This would in turn lead to additional stabilization of the inhibitor–enzyme complex. Since the aniline analogues do not possess carbonyl functional groups similar stabilizing interactions between the anilines and the MAO-A and -B active sites are absent. For the anilines, the anilinic

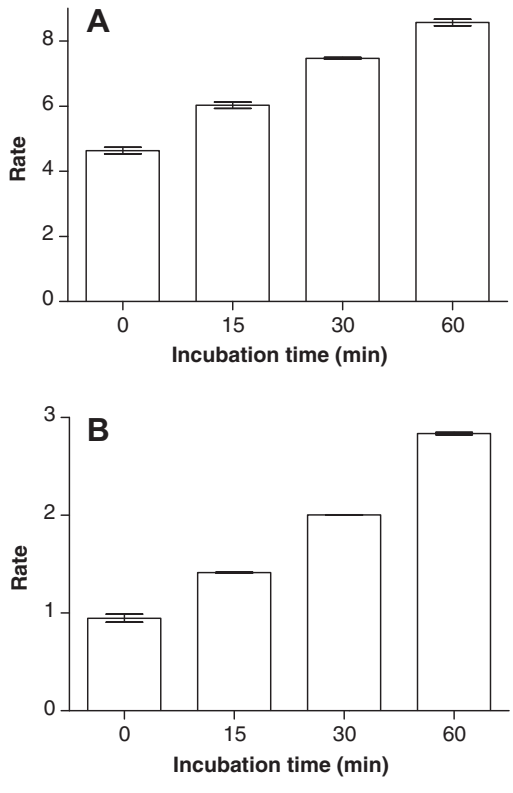


**Figure 6.** Time-dependant inhibition of the recombinant human MAO-A (Panel A) and recombinant human MAO-B (Panel B) catalysed oxidation of kynuramine by compound **9c**. The enzymes were preincubated for various periods of time (0–60 min) with **9c** at concentrations of 9.76 μM and 2.80 μM for MAO-A and MAO-B, respectively. The concentrations of kynuramine used were 45 μM and 30 μM for the studies with MAO-A and MAO-B, respectively, and the rate data are expressed as nmol 4-hydroxyquinoline formed/min/mg protein. The catalytic rates recorded in the absence of the inhibitors are 12.6 ± 1.05 and 6.94 ± 0.02 nmol/min/mg for MAO-A and -B, respectively.

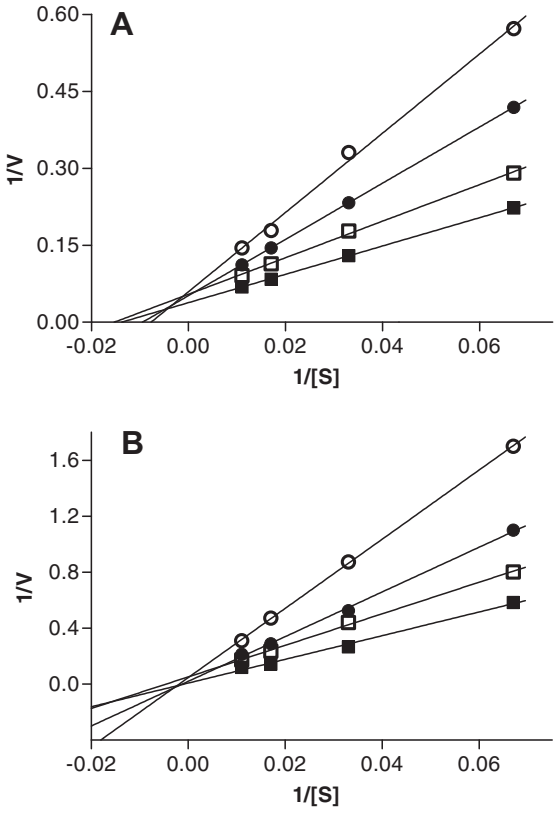


**Figure 7.** Lineweaver–Burk plots of the recombinant human MAO-A (Panel A) and recombinant human MAO-B (Panel B) catalysed oxidation of kynuramine in the absence (filled squares) and presence of various concentrations of **9c**. For the studies with MAO-A (Panel A) the concentrations of **9c** were: 2.5 μM (open squares), 5 μM (filled circles), 10 μM (open circles). For the studies with MAO-B (Panel B) the concentrations of **9c** were: 0.125 μM (open squares), 0.25 μM (filled circles), 0.5 μM (open circles). The rates (*V*) are expressed as nmol product formed/min/mg protein.

nitrogen is the only functional group that could undergo hydrogen bonding in the vicinity of the FAD co-factor. To provide additional insight, the binding modes of 5-benzyloxyisatin (**9a**) and its corresponding aniline, 4-benzyloxyaniline (**10a**), in MAO-A and -B were examined using molecular docking.

The structures of human MAO-A co-crystallized with harmine (PDB entry: 2Z5X)[3] and human MAO-B co-crystallized with safinamide (PDB entry: 2V5Z)[22] were selected and molecular docking was carried out according to a modification of a previously reported protocol with the LigandFit application of the Discovery Studio 1.7 modelling software (Accelrys).[21] These models were selected based on the high resolution of the crystallographic structures. Furthermore, in the complex between MAO-B and safinamide, the side chain of Ile-199 is rotated out of the normal conformation. This allows for the fusion of the entrance and substrate cavities which is a necessity for the binding of relatively large inhibitors which span both the entrance and substrate cavities.[16] The active site of MAO-A on the other hand consists of a single cavity. The valences of the FAD co-factor and the co-crystallised ligands were corrected, hydrogen atoms were added to the MAO-A and -B models and the models were subjected to a three-step energy minimisation procedure with the protein backbone constrained (see Section 4). After the energy minimisation procedure, the backbone constraint was removed and the co-crystallised ligands were deleted from the models. The structures of **9a** and **10a** were constructed and geometry optimised within Discovery Studio and subsequently docked into the protein models with the LigandFit application of Discovery Studio. The docked inhibitor orientations and conformations were further refined with the Smart Minimizer algorithm in Discovery Studio and 10 possible binding solutions were computed for each inhibitor. The accuracy of this procedure was evaluated by redocking the co-crystallized ligands, harmine and safinamide, into the active sites of MAO-A and -B, respectively. After each inhibitor was docked three times the best-ranked orientations of harmine and safinamide exhibited RMSD values of 0.64 Å and 1.54 Å, respectively, from the position of the co-crystallized ligand. This protocol was therefore deemed to be suitable for the docking of inhibitors into the active site of MAO-B.

The best-ranked docking solution of isatin derivative **9a** within the active site of MAO-B shows that the dioxoindolyl ring binds within the substrate cavity in close proximity of the FAD co-factor (Fig. 8A). This binding orientation of the dioxoindolyl ring is similar to that observed for isatin co-crystallized within the active site of recombinant human MAO-B[17] and for (*E*)-5-styrylisatin previously docked into an MAO-B model.[18] The C5 benzyloxy side chain of **9a** extends beyond the boundary defined by the side chain of Ile-199 into the entrance cavity of the enzyme. This binding orientation is similar to that observed for the co-crystallized inhibitor, safinamide, which also spans both active site cavities.[22] A variety of relatively large inhibitors such as *trans*,*trans*-farnesol[16] and 1,4-diphenyl-2-butene[17] are also reported to traverse both MAO-B active site cavities. Within the hydrophobic environment of the entrance cavity, the benzyloxy side chain is most likely stabilized by Van der Waals interactions.[31] These interactions may, in part, explain the enhanced MAO-B inhibition potencies of C5- and C6-substituted isatin analogues compared to isatin (Table 2). In contrast to the substituted isatin analogues, isatin binds only within the substrate cavity and does not interact with the entrance cavity residues. Of importance is the observation that the 2-oxo and NH functional groups of **9a** interact via hydrogen bonding with water molecules present in the active site. In the three-dimensional structure of isatin bound to human MAO-B, the C2 carbonyl oxygen of isatin is also hydrogen bonded to an ordered water molecule in the substrate cavity.[17] The NH functional group may also undergo hydrogen bonding with the phenolic OH of Tyr-435. Another

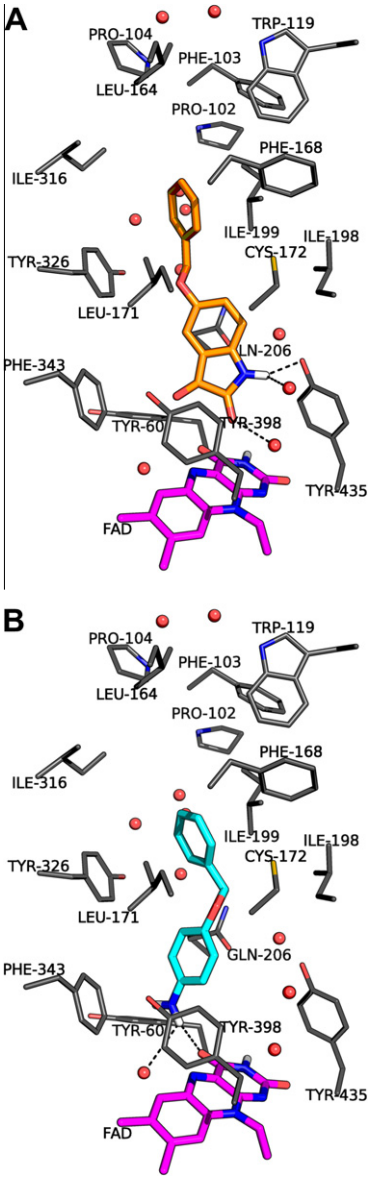


**Figure 8.** Representation of the best-ranked docking solution for the binding of isatin analogue **9a** (orange coloured, Panel A) and aniline analogue **10** (cyan coloured, Panel B) in the active site of MAO-B (2V5Z.pdb).[22] The illustrations were generated with PyMOL.[41]

significant interaction between **9a** and the MAO-B active site is a possible π–π interaction between the isatin ring and the amide functional group of the Gln-206 side chain with an interplane distance of approximately 3.5 Å[3]. As discussed above, this interaction may also, in part, explain the enhanced binding affinity of the isatin analogues to MAO-B compared to the aniline analogues.

In the best-ranked docking solution of aniline derivative **10a** within the active site of MAO-B, the $NH_2$ functional group binds in the polar region of the substrate cavity in the vicinity of the FAD co-factor and the 'aromatic sandwich' defined by Tyr-398 and Tyr-435 (Fig. 8B). This is consistent with the proposal that the $NH_2$ moiety of aminyl substrates of MAO-B is recognised by the same aromatic residues.[34] Within the substrate cavity, the $NH_2$ functional group possibly forms hydrogen bonds with a water molecule and the C4 carbonyl oxygen of the flavin. Similar to what has been observed for the MAO-B–**9a** complex, the benzyloxy side chain of **10a** also extends towards the entrance cavity of the enzyme where it is possibly stabilized via Van der Waals interactions.

One of the most notable differences between the binding modes of **9a** and **10a** within the MAO-B active site is the presence of the additional hydrogen bond interaction between the 2-oxo group of **9a** and a water molecule. In accordance with the analysis above, this interaction may, in part, explain the enhanced MAO-B inhibition potencies of the isatin analogues compared to the corresponding aniline analogues.

Examination of the binding modes of **9a** (Fig. 9A) and **10a** (Fig. 9B) within the MAO-A active site, reveals that these inhibitors adopt similar orientations to those observed in the MAO-B active site. The isatin ring of **9a** is located in close proximity to the FAD co-factor and both the C2 and C3 carbonyl oxygens are hydrogen bonded to active site water molecules. Interestingly, in contrast to the binding orientations of isatin[17] and **9a** in the human MAO-B active site, in the MAO-A active site, the dioxoindolyl ring of **9a** is rotated through ~180°. The dioxoindolyl ring of **9a** possibly forms a π–π interaction with the amide functional group of the Gln-215 side chain with an interplane distance of approximately 3.6 Å[3]. Inhibitor **10a**, on the other hand, is only hydrogen bonded via its anilinic $NH_2$ to a water molecule and possibly the C4 carbonyl oxygen of the flavin. The observation that the MAO-A–**9a** complex is stabilized by hydrogen bonding to both the 2- and 3-oxo groups while the MAO-A–**10a** complex is by hydrogen bonding to only the $NH_2$ may, in part, explain the enhanced MAO-A inhibition potencies of the isatin analogues compared to the corresponding aniline analogues.

## 3. Discussion

In the present study a series of 10 C5- and C6-substituted isatin analogues (**9a**–**j**) were synthesized and evaluated as MAO inhibitors. The results document that the isatin analogues are reversible competitive inhibitors of both MAO isoforms and in most instances exhibit selectivity for MAO-B (Table 2). Of the 10 analogues, only 3 compounds (**9d**, **g** and **h**) were selective for MAO-A. It can therefore be concluded that, similar to isatin (**1**), C5- and C6-substituted isatin analogues act in general as MAO-B selective inhibitors. Also noteworthy is the finding that C5- and C6-substitution of isatin in general leads to a considerable enhancement of the MAO-B inhibition potencies of the test compounds while having, with the exception of **9g**, a smaller effect on the MAO-A inhibition potencies. The results also document that, without exception, the C5-substituted isatin analogues are more potent inhibitors of MAO-A and -B than the corresponding C6-substituted isatin homologues. This finding is similar to the observation that (*E*)-5-styrylisatin (**2**) is a better MAO-A and -B inhibitor than the C6-substituted analogue (*E*)-6-styrylisatin (**3**). It can therefore be concluded that C5-substitution of isatin is more optimal than C6-substition for improving the MAO inhibition potencies of isatin. The finding that C5- and C6-substitution considerably enhances the MAO-B inhibition potency of isatin is in agreement with the view that the C5- and C6-side chains interact with the entrance cavity amino acid residues in order to allow for more productive interactions with the enzyme compared to isatin and hence more potent inhibition.

A possible explanation for the higher binding affinities of the C5-substituted isatin analogues towards MAO-B compared to MAO-A may be found by examining the docked binding modes of **9a** in the active sites of human MAO-A and -B. While the dioxoindolyl ring of **9a** adopts a similar binding orientation in MAO-B to that observed for isatin in an MAO-B–isatin X-ray crystal structure model,[17] in the MAO-A active site the dioxoindolyl ring of **9a** is rotated through approximately 180° (Fig. 10). This alternative binding orientation in the MAO-A active site may be less optimal for the formation of stabilizing interactions with the active site residues and water molecules. These results is in agreement with previous docking studies which showed that the isatin ring of

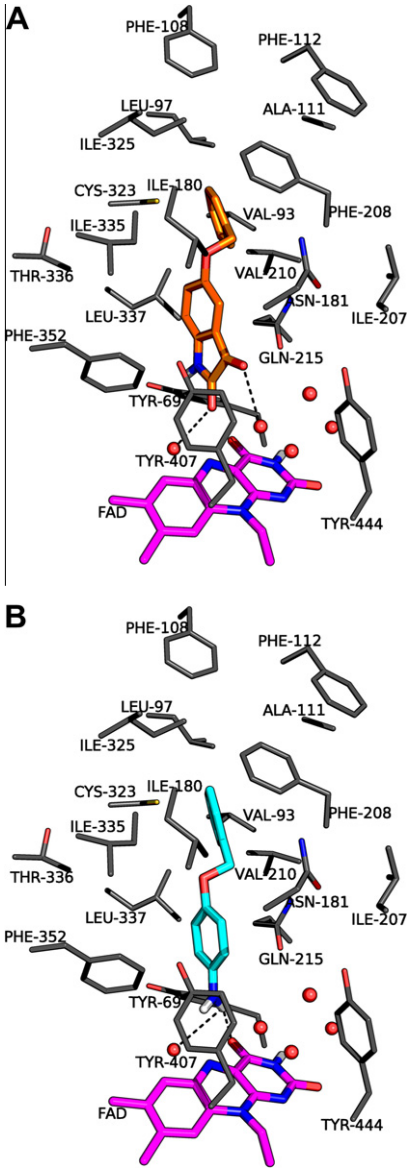


**Figure 9.** Representation of the best-ranked docking solution for the binding of isatin analogue **9a** (orange coloured, Panel A) and aniline analogue **10** (cyan coloured, Panel B) in the active site of MAO-A (2Z5X.pdb).[3] The illustrations were generated with PyMOL.[41]

(*E*)-5-styrylisatin also occupies the alternative binding orientation in the MAO-A active site[18] and suggests that other C6-substituted isatin analogues also adopts the alternative orientation in MAO-A.

A similar analysis may explain the higher binding affinities of the C5-substituted isatin analogues towards MAO-B compared to the binding affinities of the corresponding C6-substituted isatin analogues. In the docked binding mode of **9b** in the active site of human MAO-B, the dioxoindolyl ring of **9b** is also rotated through ~180° compared to the orientation of **9a** (Fig. 11). Compound **9b** therefore occupies a less optimal binding orientation in MAO-B than **9a**, and hence exhibits a lower MAO-B inhibition potency than inhibitor **9a**. This alternative binding orientation of the dioxoindolyl ring of **9b** in the MAO-B active site is similar to that observed for (*E*)-6-styrylisatin previously docked into an MAO-B model[18] and is most probably shared by other C6-substituted isatin analogues.

In this study we have also examined the importance of the isatin moiety for binding to MAO-A and MAO-B by comparing the inhibition potencies of the C5- and C6-substituted isatins with those of

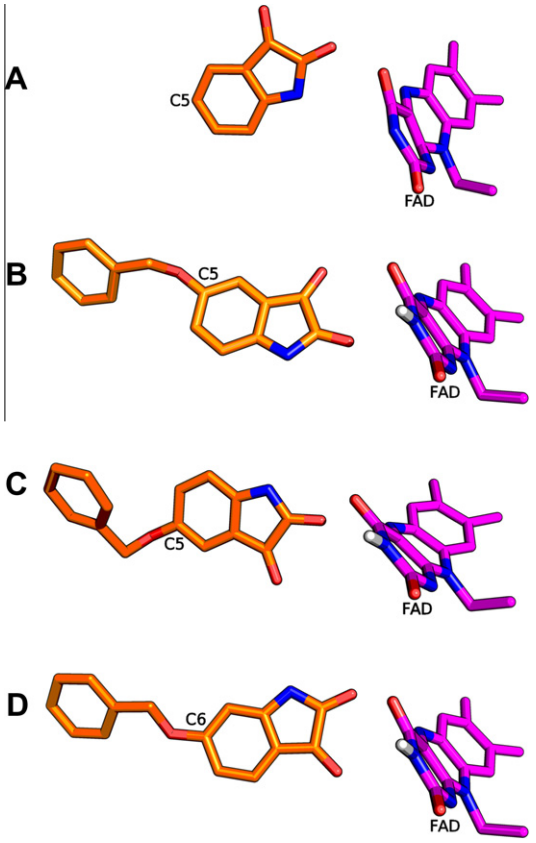


**Figure 10.** Representation of the binding orientation of isatin (Panel A) in an MAO-B–isatin X-ray crystal structure model,[17] the docked orientations of **9a** in the active sites of MAO-B (Panel B) and MAO-A (Panel C) and the docked orientation of **9b** in the MAO-B active site (Panel D).

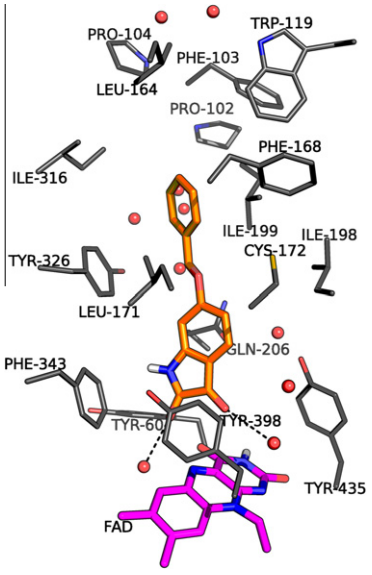


**Figure 11.** Representation of the best-ranked docking solution for the binding of isatin analogue **9b** (orange coloured) in the active site of MAO-B (2V5Z.pdb).[22] The illustration was generated with PyMOL.[41]

the corresponding aniline analogues. The results showed that the aniline analogues are weaker MAO-A and -B inhibitors than the corresponding isatin analogues and suggests that the lactam and C2 carbonyl functional groups of the dioxoindolyl ring are important structural features for binding to the MAO active sites. Molecular docking studies suggest that in both MAO-A and -B, the isatin ring forms one additional hydrogen bond interaction with the active site residues and waters of MAO-A and -B than the corresponding aniline analogues. This may, in part, explain the enhanced MAO inhibition potencies of the isatin analogues compared to the corresponding aniline analogues. Another factor that may contribute to stabilizing the complexes between the isatin analogues and the MAO isozymes are possible π–π stacking interactions between the isatin ring and the amide π-face of an active site Gln residue. In MAO-A, Gln-215 undergo stacking interactions with isatin **9a** while in MAO-B Gln-206 form stacking interactions with **9a**.

## 4. Experimental section

### 4.1. Chemicals and instrumentation

Unless otherwise noted, all starting materials were obtained from Sigma–Aldrich and were used without purification. Proton ($^1$H) and carbon ($^{13}$C) NMR spectra were recorded on a Varian Gemini 300 spectrometer at frequencies of 300 MHz and 75 MHz, respectively, and on a Bruker Avance III 600 spectrometer at frequencies of 600 MHz and 150 MHz, respectively. All NMR measurements were conducted in DMSO-*d6* and the chemical shifts are reported in parts per million ($\delta$) downfield from the signal of tetramethylsilane added to the deuterated solvent. Spin multiplicities are given as s (singlet), br s (broad singlet), d (doublet), dd (doublet of doublets), t (triplet) or m (multiplet). Direct insertion electron impact ionisation (EIMS) and high resolution mass spectra (HRMS) were obtained on a DFS high resolution magnetic sector mass spectrometer (Thermo Electron Corporation). Melting points (mp) were determined on a Stuart SMP10 melting point apparatus and are uncorrected. Column chromatography was carried out with Silica gel 60 (Fluka; 0.063–0.2 mm) while thin layer chromatography (TLC) was carried out using silica gel 60 (Merck) with $UV_{254}$ fluorescent indicator. To determine the purity of the synthesized compounds, HPLC analyses were conducted with an Agilent 1100 HPLC system equipped with a quaternary pump and an Agilent 1100 series diode array detector (see Supplementary data). HPLC grade acetonitrile (Merck) and Milli-Q water (Millipore) was used for the chromatography. For fluorescence spectrophotometry, a Varian Cary Eclipse fluorescence spectrophotometer was employed. Microsomes from insect cells containing recombinant human MAO-A and -B (5 mg/mL), kynuramine·2HBr and isatin were obtained from Sigma–Aldrich. (*E*)-5-Styrylisatin (**2**), (*E*)-6-styrylisatin (**3**), aniline **10k** and aniline **10l** were synthesized as described previously.[18] Single-crystal X-ray diffraction analysis was carried out with a Bruker Smart X2S diffractometer.

### 4.2. Synthesis of C5- and C6-substituted isatin analogues (9a–j)

The C5- and C6-substituted isatin analogues (**9a**–**j**) investigated in this study were synthesized according to a modification of the literature description.[23] A mixture of the appropriate C4- or C5-substituted aniline (**10**, 20 mmol) and acetic acid (35 mL) was heated at 110–120 °C to yield a clear solution. For this purpose either the free base or hydrochloride salt of the aniline may be used. Diethyl ketomalonate (20 mmol) was added to the reaction and the resulting solution was heated under reflux at 110–120 °C for 8 h. The residual acetic acid was removed by steam distillation and the pH of the reaction mixture was adjusted to 11 with potassium hydroxide (10%). The reaction was again heated under reflux at 120 °C for a period of 18 h while a stream of air was passed continuously through the reaction mixture. The reaction was cooled to room temperature and gravity filtered to yield a clear filtrate. The pH of the filtrate was adjusted to 3 with hydrochloric acid (20%)

and the resulting precipitate was removed by vacuum filtration. The pH of the filtrate was adjusted to <1 with hydrochloric acid (20%) and the resulting orange to red precipitate was collected by vacuum filtration. The precipitate (dissolved in ethyl acetate) was applied to a short silica gel column (35 × 80 mm) and eluted with ethyl acetate as mobile phase. Elution of the target isatin analogues were monitored by silica gel TLC using ethyl acetate/petroleum ether (50:50) as mobile phase and the plates were visualised under UV light (254 nm). The products thus obtained were recrystallized from ethyl acetate. For previously described **9g** and **9h** the melting points were found to be 208–211 °C and 231–233 °C while the reported melting points are 208–210 °C and 235 °C, respectively.[23]

#### 4.2.1. 5-Benzyloxyisatin (9a)

The title compound (bright red crystals) was prepared from 4-benzyloxyaniline hydrochloride (**10a**, Merck) and diethyl ketomalonate in a yield of 2.7%: mp 184–185 °C (ethyl acetate). $^1$H NMR (Varian Gemini 300, DMSO-*d6*) $\delta$ 5.09 (s, 2H), 6.83 (d, 1H, $J$ = 8.5 Hz), 7.14 (d, 1H, $J$ = 2.6 Hz), 7.23–7.44 (m, 6H), 10.8 (s, 1H); $^{13}$C NMR (Varian Gemini 300, DMSO-*d6*) $\delta$ 69.9, 109.9, 113.2, 118.1, 125.8, 127.7, 127.9, 128.4, 136.8, 144.8, 154.2, 159.5, 184.6; EIMS 253; HRMS *m*/*z*: calcd 253.0739, found 253.0736; purity (HPLC): 99.6%; UV ($CH_3CN$) $\lambda_{max}$ 253 nm (ε 25,900 $M^{-1}$), 298 nm (ε 2400 $M^{-1}$), 466 nm (ε 957 $M^{-1}$).

#### 4.2.2. 6-Benzyloxyisatin (9b)

The title compound (bright orange crystals) was prepared from 3-benzyloxyaniline (free base) (**10b**, Merck) and diethyl ketomalonate in a yield of 1.2%: mp 243–255 °C (decomp., ethyl acetate). $^1$H NMR (Varian Gemini 300, DMSO-*d6*) $\delta$ 5.24 (s, 2H), 6.46 (d, 1H, $J$ = 2.2 Hz), 6.64–6.67 (m, 1H), 7.32–7.49 (m, 6H), 10.96 (br s, 1H); $^{13}$C NMR (Varian Gemini 300, DMSO-*d6*) $\delta$ 70.0, 98.5, 109.5, 111.3, 127.3, 127.8, 128.2, 128.5, 136.0, 153.5, 160.5, 166.7, 181.5; EIMS 253; HRMS *m*/*z*: calcd 253.0739, found 253.0733; purity (HPLC): 99.5%; UV ($CH_3CN$) $\lambda_{max}$ 261 nm (ε 26,500 $M^{-1}$), 318 nm (ε 12,200 $M^{-1}$), 395 nm (ε 1746 $M^{-1}$).

#### 4.2.3. 5-(2-Phenylethyl)isatin (9c)

The title compound (bright red crystals) was prepared from 4-(2-phenylethyl)aniline hydrochloride (**10c**) and diethyl ketomalonate in a yield of 5.3%: mp 165–167 °C (ethyl acetate). $^1$H NMR (Varian Gemini 300, DMSO-*d6*) $\delta$ 2.82 (s, 4H), 6.80, (d, 1H, $J$ = 8.0 Hz), 7.15–7.28 (m, 5H), 7.36–7.43 (m, 2H), 10.95 (s, 1H); $^{13}$C NMR (Varian Gemini 300, DMSO-*d6*) $\delta$ 36.0, 36.9, 112.0, 117.8, 124.4, 125.9, 128.2, 128.4, 136.2, 138.4, 141.1, 148.9, 159.5, 184.5; EIMS 251; HRMS *m*/*z*: calcd 251.0946, found 251.0941; purity (HPLC): 99.5%; UV ($CH_3CN$) $\lambda_{max}$ 247 nm (ε 30,100 $M^{-1}$), 298 nm (ε 3700 $M^{-1}$), 423 nm (ε 935 $M^{-1}$).

#### 4.2.4. 6-(2-Phenylethyl)isatin (9d)

The title compound (bright orange crystals) was prepared from 3-(2-phenylethyl)aniline hydrochloride (**10d**) and diethyl ketomalonate in a yield of 4.6%: mp 203–205 °C (ethyl acetate). $^1$H NMR (Bruker Avance III 600, DMSO-*d6*) $\delta$ 2.85–2.92 (m, 4H), 6.75 (s, 1H), 6.91 (d, 1H, $J$ = 7.5 Hz), 7.17 (t, 1H, $J$ = 7.2 Hz), 7.22–7.28 (m, 4H), 7.39 (d, 1H, $J$ = 7.5 Hz), 11.00 (br s, 1H); $^{13}$C NMR (Bruker Avance III 600, DMSO-*d6*) $\delta$ 36.2, 37.7, 112.2, 115.9, 123.0, 124.7, 126.0, 128.3, 128.4, 140.9, 151.1, 153.8, 159.9, 183.7; EIMS 251; HRMS *m*/*z*: calcd 251.0946, found 251.0940; purity (HPLC): 99.8%; UV ($CH_3CN$) $\lambda_{max}$ 249 nm (ε 29,000 $M^{-1}$), 305 nm (ε 7530 $M^{-1}$), 412 nm (ε 1031 $M^{-1}$).

#### 4.2.5. 5-Phenoxyisatin (9e)

The title compound (bright red crystals) was prepared from 4-phenoxyaniline (free base) (**10e**) and diethyl ketomalonate in a yield of 9.3%: mp 185–190 °C (decomp., ethyl acetate). $^1$H NMR (Bruker Avance III 600, DMSO-*d6*) $\delta$ 6.93 (d, 1H, $J$ = 8.7 Hz), 6.98 (d, 2H, $J$ = 7.9 Hz), 7.10 (m, 1H), 7.12 (t, 1H, $J$ = 7.2 Hz), 7.29 (m, 1H), 7.37 (t, 2H, $J$ = 7.9 Hz), 11.00 (s, 1H); $^{13}$C NMR (Bruker Avance III 600, DMSO-*d6*) $\delta$ 113.6, 115.0, 118.0, 118.6, 123.5, 129.1, 130.1, 146.7, 151.9, 157.0, 159.6, 184.1; EIMS 239; HRMS *m*/*z*: calcd 239.0582, found 239.0574; purity (HPLC): 99.7%; UV ($CH_3CN$) $\lambda_{max}$ 249 nm (ε 30,100 $M^{-1}$), 294 nm (ε 2530 $M^{-1}$), 433 nm (ε 925 $M^{-1}$).

#### 4.2.6. 6-Phenoxyisatin (9f)

The title compound (bright yellow crystals) was prepared from 3-phenoxyaniline (free base) (**10f**) and diethyl ketomalonate in a yield of 3.0%: mp 146–150 °C (decomp., ethyl acetate/*n*-hexane, 1:1). $^1$H NMR (Bruker Avance III 600, DMSO-*d6*) $\delta$ 6.28 (s, 1H), 6.55 (d, 1H, $J$ = 8.7 Hz), 7.20 (d, 2H, $J$ = 8.3 Hz), 7.31 (t, 1H, $J$ = 7.15 Hz), 7.51 (m, 3H), 10.89 (br s, 1H); $^{13}$C NMR (Bruker Avance III 600, DMSO-*d6*) $\delta$ 99.9, 110.9, 112.5, 120.9, 125.8, 127.5, 130.5, 153.4, 153.8, 160.1, 166.0, 181.8; EIMS 239; HRMS *m*/*z*: calcd 239.0582, found 239.0582; purity (HPLC): 99.4%; UV ($CH_3CN$) $\lambda_{max}$ 256 nm (ε 22,100 $M^{-1}$), 316 nm (ε 11,300 $M^{-1}$), 394 nm (ε 1667 $M^{-1}$).

#### 4.2.7. 5-Phenylisatin (9g)

The title compound (bright red crystals) was prepared from 4-aminobiphenyl (free base) (**10g**) and diethyl ketomalonate in a yield of 8.5%: mp 208–211 °C (ethyl acetate), lit. mp 208–210 °C.[23] $^1$H NMR (Bruker Avance III 600, DMSO-*d6*) $\delta$ 6.97 (d, 1H, $J$ = 8.3 Hz), 7.34 (t, 1H, $J$ = 7.5 Hz),7.43 (t, 2H, $J$ = 7.5 Hz), 7.61 (d, 2H, $J$ = 7.5 Hz), 7.72 (d, 1H, $J$ = 1.5 Hz), 7.86 (dd, 1H, $J$ = 1.9, 8.3 Hz), 11.13 (br s, 1H); $^{13}$C NMR (Bruker Avance III 600, DMSO-*d6*) $\delta$ 112.7, 118.4, 122.5, 126.2, 127.5, 129.0, 134.9, 136.5, 138.7, 150.0, 159.6, 184.4; EIMS 223; HRMS *m*/*z*: calcd 223.0633, found 223.0632; purity (HPLC): 99.8%; UV ($CH_3CN$) $\lambda_{max}$ 260 nm (ε 44,700 $M^{-1}$), 430 nm (ε 981 $M^{-1}$).

#### 4.2.8. 6-Phenylisatin (9h)

The title compound (orange-red crystals) was prepared from 3-aminobiphenyl (free base) (**10h**) and diethyl ketomalonate in a yield of 3.7%: mp 231–233 °C (ethyl acetate), lit. mp 235 °C.[23] $^1$H NMR (Bruker Avance III 600, DMSO-*d6*) $\delta$ 7.09 (s, 1H), 7.34 (d, 1H, $J$ = 7.5 Hz), 7.46 (t, 1H, $J$ = 7.2 Hz), 7.51 (t, 2H, $J$ = 7.2 Hz), 7.57 (d, 1H, $J$ = 7.5 Hz), 7.69 (d, 2H, $J$ = 7.5 Hz), 11.14 (s, 1H); $^{13}$C NMR (Bruker Avance III 600, DMSO-*d6*) $\delta$ 110.1, 116.8, 121.3, 125.3, 127.1, 129.1, 129.2, 138.9, 149.9, 151.4, 159.8, 183.7; EIMS 223; HRMS *m*/*z*: calcd 223.0633, found 223.0628; purity (HPLC): 98.3%; UV ($CH_3CN$) $\lambda_{max}$ 266 nm (ε 15,360 $M^{-1}$), 326 nm (ε 15,860 $M^{-1}$), 408 nm (ε 1578 $M^{-1}$).

#### 4.2.9. 5-(4-Phenylbutyl)isatin (9i)

The title compound (dark red crystals) was prepared from 4-(4-phenylbutyl)aniline hydrochloride (**10i**) and diethyl ketomalonate in a yield of 5.0%: mp 116–121 °C (ethyl acetate). $^1$H NMR (Bruker Avance III 600, DMSO-*d6*) $\delta$ 1.52 (m, 4H), 3.41 (m, 4H), 6.80 (d, 1H, $J$ = 7.9 Hz), 7.14 (d, 3H, $J$ = 7.5 Hz), 7.23 (t, 2H, $J$ = 7.5 Hz), 7.28 (s, 1H), 7.37 (d, 1H, $J$ = 7.9 Hz), 10.95 (s, 1H); $^{13}$C NMR (Bruker Avance III 600, DMSO-*d6*) $\delta$ 30.4, 30.5, 34.0, 34.9, 112.1, 117.8, 124.2, 125.7, 128.26, 128.28, 136.9, 138.3, 142.1, 148.8, 159.5, 184.6; EIMS 279; HRMS *m*/*z*: calcd 279.1259, found 239.1253; purity (HPLC): 99.7%; UV ($CH_3CN$) $\lambda_{max}$ 247 nm (ε 27,300 $M^{-1}$), 298 nm (ε 3400 $M^{-1}$), 423 nm (ε 955 $M^{-1}$).

#### 4.2.10. 5-(4-Chlorophenoxy)isatin (9j)

The title compound (bright red crystals) was prepared from 4-(4-chlorophenoxy)aniline (free base) (**10j**) and diethyl ketomalonate in a yield of 5.2%: mp 255–257 °C. $^1$H NMR (Bruker Avance III 600, DMSO-*d6*) $\delta$ 6.93(d, 1H, $J$ = 8.3 Hz), 6.99 (d, 2H, $J$ = 9.0 Hz), 7.16 (d, 1H, $J$ = 2.6 Hz), 7.31 (dd, 1H, $J$ = 2.6, 8.7 Hz), 7.40 (d, 2H,

$J$ = 8.7 Hz), 11.05 (s, 1H); $^{13}$C NMR (Bruker Avance III 600, DMSO-*d6*) $\delta$ 113.7, 115.5, 118.7, 119.5, 127.1, 129.4, 129.9, 147.0, 151.4, 156.1, 159.5, 184.0; EIMS 273; HRMS *m*/*z*: calcd 273.0193, found 273.0192; purity (HPLC): 99.4%; UV ($CH_3CN$) $\lambda_{max}$ 249 nm ($\varepsilon$ 34,400 $M^{-1}$), 430 nm ($\varepsilon$ 980 $M^{-1}$).

### 4.3. Synthesis of aniline analogues

With the exception of **10c**, **10d** and **10i** all the anilines required for the synthesis of the isatin analogues were commercially available. Sodium (105 mmol) was allowed to react with ethanol (109 mL) in small portions over a period of 2 h. The resulting mixture was added at room temperature to diethyl 4- or diethyl 3-nitrobenzylphosphonate (**11a**, **b**, 100 mmol)[26] and benzaldehyde (**12**, 100 mmol) or cinnamaldehyde (**14**, 100 mmol) dissolved in ethanol (164 mL) over a period of 1.5 h. Stirring was continued for 20 h and the thick yellow precipitate was collected by vacuum filtration and washed with 40 mL ethanol followed by 40 mL petroleum ether.[27] The nitro-functionalized intermediates **13a**, **13b** and **15** thus obtained (yield 69–71%) were used without further purification in the following reaction. The nitro derivatives (25 mmol) were suspended in 400 mL methanol and the reaction flask was purged with argon. A quantity of 3% (of the weight of the nitro derivative) of Pd/C (10%) was prewet with 2 mL water and added to 10 mL methanol. This mixture was carefully added to the reaction. The atmosphere was replaced by hydrogen and the reaction was stirred at room temperature for 24 h during which the reaction became a clear solution. The catalyst was removed by filtration through a bed of Celite and the methanol solvent was evaporated under reduced pressure. The resulting aniline derivative was converted to the corresponding hydrochloride salt in $CH_2Cl_2$ (70 mL). A volume of 150 mL diethyl ether may be added to the acidic $CH_2Cl_2$ solution to facilitate precipitation of the salt (yield 41–95%). The melting points of the hydrochloride salts of **10c**, **10d** and **10i** were found to be 203–210 °C (decomp.), 164–181 °C and 174–180 °C, respectively.

#### 4.3.1. Hydrochloride salt of 4-(2-phenylethyl)aniline (10c)

The title compound was prepared from 4-nitrostilbene (**13a**) in a yield of 94.9%: mp 203–210 °C (decomp.), lit. mp 210 °C.[35,36] $^1$H NMR (Varian Gemini 300, DMSO-*d6*) $\delta$ 2.87 (m, 4H), 7.13–7.33 (m, 9H), 10.39 (br s, 3H); $^{13}$C NMR (Varian Gemini 300, DMSO-*d6*) $\delta$ 36.4, 36.8, 123.0, 125.9, 128.2, 128.4, 129.56, 129.62, 141.1, 141.4; EIMS 197.

#### 4.3.2. Hydrochloride salt of 3-(2-phenylethyl)aniline (10d)

The title compound was prepared from 3-nitrostilbene (**13b**) in a yield of 65.1%: mp 164–181 °C (methanol/ethyl acetate, 1:2).[36] $^1$H NMR (Bruker Avance III 600, DMSO-*d6*) $\delta$ 2.84–2.91 (m, 4H), 7.16 (t, 1H, $J$ = 7.2 Hz), 7.21–7.27 (m, 7H), 7.36 (t, 1H, $J$ = 7.5 Hz), 10.50 (br s, 3H); $^{13}$C NMR (Bruker Avance III 600, DMSO-*d6*) $\delta$ 36.6, 36.7, 120.8, 123.0, 126.0, 128.1, 128.3, 128.4, 129.5, 131.9, 141.1, 143.4; EIMS 197.

#### 4.3.3. Hydrochloride salt of 4-(4-phenylbutyl)aniline (10i)

The title compound was prepared from 1-nitro-4-[(1*E*,3*E*)-4-phenylbuta-1,3-dien-1-yl]benzene (**15**) in a yield of 40.9%: mp 174–180 °C (methanol/ethyl acetate, 1:1).[37] $^1$H NMR (Varian Gemini 300, DMSO-*d6*) $\delta$ 1.55 (m, 4H), 2.57 (m, 4H), 7.11–7.31 (m, 9H), 10.41 (br s, 3H); $^{13}$C NMR (Varian Gemini 300, DMSO-*d6*) $\delta$ 30.5, 30.6, 34.3, 34.9, 123.1, 125.6, 128.3, 129.42, 129.45, 142.1, 142.2; EIMS 225.

### 4.4. Recombinant human MAO-A and -B inhibition studies

Microsomes prepared from insect cells expressing recombinant human MAO-A and -B (5 mg/mL) were obtained from Sigma–Aldrich and were pre-aliquoted and stored at −70 °C. All enzymatic reactions were carried out to a final volume of 500 μL in potassium phosphate buffer (100 mM, pH 7.4, made isotonic with KCl, 20.2 mM) and contained kynuramine as substrate, MAO-A or MAO-B (0.0075 mg/mL) and various concentrations of the test inhibitor (0–100 μM). The final concentrations of kynuramine in the reactions were 45 μM and 30 μM where MAO-A and -B, respectively, were used as enzymes. Stock solutions of the test inhibitors were prepared in DMSO and added to the reactions to yield a final concentration of 4% (v/v) DMSO. The reactions were carried out for 20 min at 37 °C and were terminated with the addition of 200 μL NaOH (2 N). After the addition of distiled water (1200 μL) to each reaction, the reactions were centrifuged for 10 minutes at 16,000*g*. To determine the concentrations of the MAO-generated 4-hydroxyquinoline in the reactions, the fluorescence of the supernatant at an excitation wavelength of 310 nm and an emission wavelength of 400 nm were measured.[28] Quantitative estimations of 4-hydroxyquinoline were made with the aid of a linear calibration curve ranging from 0.047 to 1.56 μM of the reference standard dissolved in potassium phosphate buffer (100 mM, pH 7.4). Each calibration standard was prepared to a final volume of 500 μL in potassium phosphate buffer (100 mM, pH 7.4) and contained 4% DMSO. To each standard was also added 200 μL NaOH (2 N) and 1200 μL distiled water. $IC_{50}$ values were determined by plotting the initial rate of oxidation versus the logarithm of the inhibitor concentration to obtain a sigmoidal dose–response curve. For this purpose, nine different inhibitor concentrations spanning at least three orders of a magnitude were used for each sigmoidal curve. This kinetic data were fitted to the one site competition model incorporated into the Prism software package (GraphPad) and the $IC_{50}$ values were determined in duplicate and are expressed as mean ± standard deviation (SD).[21] The $IC_{50}$ values were converted to the corresponding $K_i$ values according to the equation by Cheng and Prusoff: $K_i = IC_{50}/(1 + [S]/K_m)$.[29]

### 4.5. Time-dependant inhibition studies

To investigate whether the observed enzyme inhibition is reversible or irreversible, time-dependant inhibition studies were carried with a selected inhibitor, **9c**. Recombinant human MAO-A or human MAO-B (0.03 mg/mL) were preincubated for periods of 0, 15, 30, 60 min at 37 °C with compound **9c**. The concentrations of inhibitor **9c** in these incubations were 9.76 μM and 2.80 μM for the incubations with MAO-A and MAO-B, respectively. These concentrations are twofold the measured $IC_{50}$ values for the inhibition of the respective MAO preparations by **9c** and the incubations were carried out in potassium phosphate buffer (100 mM, pH 7.4, made isotonic with KCl). A final concentration of 45 μM kynuramine for MAO-A and 30 μM kynuramine for MAO-B were then added to the preincubated enzyme preparations and the resulting reactions were incubated at 37 °C for 15 min. The final volumes of these incubations were 500 μL and the final concentrations of **9c** were 4.88 μM and 1.40 μM for MAO-A and MAO-B, respectively. These concentrations of the inhibitor are approximately equal to the $IC_{50}$ values for the inhibition of the respective enzyme preparations by **9c**. The final enzyme concentrations of the MAO preparations were 0.015 mg/mL. The reactions were terminated with 200 μL NaOH (2 N) and a volume of 1200 μL distiled water was added to each reaction. The rates of formation of 4-hydroxyquinoline were measured and quantified as described above. All measurements were carried out in triplicate and are expressed as mean ± SD.[21,38,39]

### 4.6. Mode of inhibition

To examine the modes of MAO-A and -B inhibition, sets of Lineweaver–Burk plots were constructed for the inhibition of both

enzymes by a selected representative inhibitor, compound **9c**. For this purpose the initial rates of oxidation of kynuramine at four different substrate concentrations (15–90 μM) in the absence and presence of three different concentrations of the inhibitor were measured. The concentrations of inhibitor **9c** were 2.5–10 μM and 0.125–0.5 μM for the inhibition studies with MAO-A and -B, respectively, while the concentration of the MAO preparation in the incubations were 0.015 mg/mL. The enzymatic reactions and measurements were carried out as described above. Linear regression analysis was performed using the Prism software package.[21]

### 4.7. Molecular modelling studies

The molecular docking studies were carried out in the Windows based Discovery Studio 1.7 molecular modelling software.[40] The ligands to be docked (**9a**, **9b** and **10**) were constructed Discovery Studio and the hydrogen atoms were added according to the appropriate protonation states at pH 7. The geometries were briefly optimised in Discovery Studio using a fast Dreiding-like forcefield (1000 iterations) and atom potential types and partial charges were subsequently automatically assigned with the Momany and Rone CHARMm forcefield. The X-ray crystallographic structures of MAO-A co-crystallized with harmine (PDB code: 2Z5X)[3] and MAO-B co-crystallized with safinamide (PDB code: 2V5Z)[22] were retrieved from the Brookhaven Protein Data Bank (www.rcsb.org/pdb). Hydrogen atoms were added to the receptor models according to the appropriate protonation states of the ionizable amino acids at pH 7. The valences of the FAD co-factors (oxidised state) and co-crystallized ligands were also corrected and hydrogen atoms were added according to the appropriate protonation states at pH 7. The resulting models were automatically typed with the Momany and Rone CHARMm forcefield, the protein backbone was constrained and the models were subjected to a three step energy minimisation cascade. The first step was a steepest descent minimisation which was followed by conjugate gradient minimisation. For both protocols the termination criteria was set to a maximum of 2500 steps or a minimum value of 0.1 for the root mean square of the energy gradient. The third step was an adopted basis Newton–Rapheson minimisation with the termination criteria set to a maximum of 5000 steps or a minimum value for the root mean square of the energy gradient of 0.01. For this minimisation cascade the implicit generalised Born solvation model with simple switching was used with the dielectric constant set to 4. The models were subsequently deprived of the co-crystallized ligands and the backbone constraints and the binding site was identified by a flood-filling algorithm. All crystal waters were retained for the modelling studies and include the water molecules which are involved in hydrogen bonding with the C2 carbonyl oxygen of isatin as shown by the crystal structure of isatin in complex with MAO-B.[17] Automated docking was subsequently carried out with the LigandFit application of Discovery Studio and 10 docking solutions were allowed for each ligand. The docking protocol uses total ligand flexibility whereby the final ligand conformations are determined by the Monte Carlo conformation search method set to a variable number of trial runs. The docked ligands were further refined using in situ ligand minimisation with the Smart Minimizer algorithm. Unless otherwise specified (see above), all the application modules within Discovery Studio were set to their default values.[21] The illustrations were generated in PyMOL.[41]

### 4.8. Single-crystal X-ray diffraction analysis

X-ray diffraction data were collected on a Bruker Smart X2S diffractometer using monochromated (doubly curved silicon crystal) Mo Kα-radiation (0.71073 Å) and employing ω scan mode. For this purpose, orange coloured crystals of compound **9d** was mounted on a Mitegen Micromount with a small amount of epoxy. Bruker APEX2 software was used for preliminary determination of the unit cell and the determination of integrated intensities and unit cell refinement were performed with Bruker SAINT system. The data were corrected for absorption effects with SADABS using the multiscan technique. The structure was solved with XS[42] and subsequent structure refinements were performed with XL.[42] The structure was refined by anisotropic full-matrix least-squares refinement on $F^2$: $C_{16}H_{13}NO_2$, $M = 251.28$ g mol$^{-1}$, crystal size: $0.05 \times 0.5 \times 0.5$ mm$^3$, orthorhombic, space group *P21 21 21*, $a = 4.7763(10)$ Å, $b = 9.835(3)$ Å, $c = 27.125(7)$ Å, $\alpha = \beta = \gamma = 90°$, $V = 1274.2(5)$ Å$^3$, $Z = 4$, $\rho_{calcd} = 1.310$ g cm$^{-3}$, $\mu = 0.087$ mm$^{-1}$, $\lambda = 0.71073$ Å, $T = 300(2)$ K, $\theta_{range} = 1.50–20.19°$, reflections collected: 5430, independent: 1234 ($R_{int} = 0.0371$), 172 parameters, final $R$ indices [$I > 2\sigma(I)$]: $R_1 = 0.0417$; $wR_2 = 0.1142$, max/min residual electron density: 0.168/−0.211 e$^-$/Å$^3$, goodness-of-fit on $F^2$ 1.105, $F(0\,0\,0) = 528$. CCDC 794009 contains the supplementary crystallographic data for this paper. These data can be obtained free of charge from The Cambridge Crystallographic Data Centre via www.ccdc.cam.ac.uk.

### Acknowledgements

The NMR and MS spectra and X-ray diffraction data were recorded by André Joubert and Johan Jordaan of the SASOL Centre for Chemistry, North-West University. This work was supported by grants from the National Research Foundation and the Medical Research Council, South Africa.

### Supplementary data

Supplementary data associated with this article can be found, in the online version, at doi:10.1016/j.bmc.2010.11.028.

### References and notes

1. Binda, C.; Newton-Vinson, P.; Hubálek, F.; Edmondson, D. E.; Mattevi, A. *Nat. Struct. Biol.* **2002**, *9*, 22.
2. Shih, J. C.; Chen, K.; Ridd, M. J. *Annu. Rev. Neurosci.* **1999**, *22*, 197.
3. Son, S.-Y.; Ma, J.; Kondou, Y.; Yoshimura, M.; Yamashita, E.; Tsukihara, T. *Proc. Natl. Acad. Sci. U.S.A.* **2008**, *105*, 5739.
4. Youdim, M. B. H.; Edmondson, D.; Tipton, K. F. *Nat. Rev. Neurosci.* **2006**, *7*, 295.
5. Gnerre, C.; Catto, M.; Leonetti, F.; Weber, P.; Carrupt, P.-A.; Altomare, C.; Carotti, A.; Testa, B. *J. Med. Chem.* **2000**, *43*, 4747.
6. Chimenti, F.; Fioravanti, R.; Bolasco, A.; Chimenti, P.; Secci, D.; Rossi, F.; Yáñez, M.; Orallo, F.; Ortuso, F.; Alcaro, S. *J. Med. Chem.* **2009**, *52*, 2818.
7. Zisook, S. E. *Psychosomatics* **1985**, *26*, 240.
8. Youdim, M. B. H.; Collins, G. G. S.; Sandler, M.; Bevan-Jones, A. B.; Pare, C. M.; Nicholson, W. J. *Nature* **1972**, *236*, 225.
9. Collins, G. G. S.; Sandler, M.; Williams, E. D.; Youdim, M. B. H. *Nature* **1970**, *225*, 817.
10. Di Monte, D. A.; DeLanney, L. E.; Irwin, I.; Royland, J. E.; Chan, P.; Jakowec, M. W.; Langston, J. W. *Brain Res.* **1996**, *738*, 53.
11. Finberg, J. P.; Wang, J.; Bankiewich, K.; Harvey-White, J.; Kopin, I. J.; Goldstein, D. S. *J. Neural Transm. Suppl.* **1998**, *52*, 279.
12. Fernandez, H. H.; Chen, J. J. *Pharmacotherapy* **2007**, *27*, 174S.
13. Youdim, M. B. H.; Bakhle, Y. S. *Br. J. Pharmacol.* **2006**, *147*, S287.
14. Nicotra, A.; Pierucci, F.; Parvez, H.; Senatori, O. *Neurotoxicology* **2004**, *25*, 155.
15. Fowler, J. S.; Volkow, N. D.; Wang, G. J.; Logan, J.; Pappas, N.; Shea, C.; MacGregor, R. *Neurobiol. Aging* **1997**, *18*, 431.
16. Hubálek, F.; Binda, C.; Khalil, A.; Li, M.; Mattevi, A.; Castagnoli, N., Jr.; Edmondson, D. E. *J. Biol. Chem.* **2005**, *280*, 15761.
17. Binda, C.; Li, M.; Hubálek, F.; Restelli, N.; Edmondson, D. E.; Mattevi, A. *Proc. Natl. Acad. Sci. U.S.A.* **2003**, *100*, 9750.
18. Van der Walt, E. M.; Milczek, E. M.; Malan, S. F.; Edmondson, D. E.; Castagnoli, N., Jr.; Bergh, J. J.; Petzer, J. P. *Bioorg. Med. Chem. Lett.* **2009**, *19*, 2509.
19. Vlok, N.; Malan, S. F.; Castagnoli, N., Jr.; Bergh, J. J.; Petzer, J. P. *Bioorg. Med. Chem.* **2006**, *14*, 3512.
20. Pretorius, J.; Malan, S. F.; Castagnoli, N., Jr.; Bergh, J. J.; Petzer, J. P. *Bioorg. Med. Chem.* **2008**, *16*, 8676.
21. Strydom, B.; Malan, S. F.; Castagnoli, N.; Bergh, J. J.; Petzer, J. P. *Bioorg. Med. Chem.* **2010**, *18*, 1018.
22. Binda, C.; Wang, J.; Pisani, L.; Caccia, C.; Carotti, A.; Salvati, P.; Edmondson, D. E.; Mattevi, A. *J. Med. Chem.* **2007**, *50*, 5848.

23. Langenbeck, V. W.; Rühlmann, K.; Reif, H. H.; Stolze, F. *J. Prakt. Chem.* **1957**, *4*, 136.
24. Da Silva, J. F. M.; Garden, S. J.; Pinto, A. C. *J. Braz. Chem. Soc.* **2001**, *12*, 273.
25. Gassman, P. G.; Cue, B. W.; Luh, T.-Y. *J. Org. Chem.* **1977**, *42*, 1344.
26. Lee, Y.-B.; Woo, H. Y.; Yoon, C.-B.; Shim, H.-K. *J. Mater. Chem.* **1999**, *9*, 2345.
27. Kuo, E. A.; Hambleton, P. T.; Kay, D. P.; Evans, P. L.; Matharu, S. S.; Little, E.; McDowall, N.; Jones, C. B.; Hedgecock, C. J.; Yea, C. M.; Chan, A. W.; Hairsine, P. W.; Ager, I. R.; Tully, W. R.; Williamson, R. A.; Westwood, R. *J. Med. Chem.* **1996**, *39*, 4608.
28. Novaroli, L.; Reist, M.; Favre, E.; Carotti, A.; Catto, M.; Carrupt, P. A. *Bioorg. Med. Chem.* **2005**, *13*, 6212.
29. Cheng, Y. C.; Prusoff, W. H. *Biochem. Pharmacol.* **1973**, *22*, 3099.
30. Van den Berg, D.; Zoellner, K. R.; Ogunrombi, M. O.; Malan, S. F.; Terre'Blanche, G., ; Castagnoli, N., Jr.; Bergh, J. J.; Petzer, J. P. *Bioorg. Med. Chem.* **2007**, *15*, 3692.
31. Novaroli, L.; Daina, A.; Favre, E.; Bravo, J.; Carotti, A.; Leonetti, F.; Catto, M.; Carrupt, P. A.; Reist, M. *J. Med. Chem.* **2006**, *49*, 6264.
32. Miller, J. R.; Edmondson, D. E. *Biochemistry* **1999**, *38*, 13670.
33. Casey, L. A.; Galt, R.; Page, M. I. *J. Chem. Soc., Perkin Trans. 2* **1993**, 23.
34. Binda, C.; Mattevi, A.; Edmondson, D. E. *J. Biol. Chem.* **2002**, *277*, 23973.
35. Braun, V. J.; Deutsch, H.; Koscielski, O. *Chem. Ber.* **1913**, *46*, 1511.
36. Carrigan, C. N.; Bartlett, R. D.; Esslinger, C. S.; Cybulski, K. A.; Tongcharoensirikul, P.; Bridges, R. J.; Thompson, C. M. *J. Med. Chem.* **2002**, *45*, 2260.
37. Bergmann, F.; Schapiro, D. *J. Org. Chem.* **1947**, *12*, 57.
38. Ogunrombi, M. O.; Malan, S. F.; Terre'Blanche, G.; Castagnoli, N., Jr.; Bergh, J. J.; Petzer, J. P. *Bioorg. Med. Chem.* **2008**, *16*, 2463.
39. Manley-King, C. I.; Terre'Blanche, G.; Castagnoli, N., Jr.; Bergh, J. J.; Petzer, J. P. *Bioorg. Med. Chem.* **2009**, *17*, 3104.
40. Accelrys Discovery Studio 1.7, Accelrys Software Inc., San Diego, CA, USA, 2006, http://www.accelrys.com.
41. DeLano, W. L. Palo Alto, CA, USA, 2002.
42. Sheldrick, G. M. *Acta Crystallogr., Sect. A* **2008**, *64*, 112.